Fidelity of Mispair Formation and Mispair Extension Is Dependent on the Interaction between the Minor Groove of the Primer Terminus and Arg668 of DNA Polymerase I of *Escherichia coli*†

Melodie D. McCain, Aviva S. Meyer, Sherri S. Schultz, Athanasios Glekas, and Thomas E. Spratt*

American Health Foundation Cancer Center, Institute for Cancer Prevention, One Dana Road, Valhalla, New York 10595

Received December 3, 2004; Revised Manuscript Received February 3, 2005

ABSTRACT: The hydrogen bonding interactions between the Klenow fragment of *Escherichia coli* DNA polymerase I with the proofreading exonuclease inactivated (KF^-) and the minor groove of DNA were examined with modified oligodeoxynucleotides in which 3-deazaguanine (3DG) replaced guanine. This substitution would prevent a hydrogen bond from forming between the polymerase and that one site on the DNA. If the hydrogen bonding interaction were important, then we should observe a decrease in the rate of reaction. The steady-state and pre-steady-state kinetics of DNA replication were measured with 10 different oligodeoxynucleotide duplexes in which 3DG was placed at different positions. The largest decrease in the rate of replication was observed when 3DG replaced guanine at the 3′-terminus of the primer. The effect of this substitution on mispair extension and formation was then probed. The G to 3DG substitution at the primer terminus decreased the k_{pol} for the extension past G/C, G/A, and G/G base pairs but not the G/T base pair. The G to 3DG substitution at the primer terminus also decreased the formation of correct base pairs as well as incorrect base pairs. However, in all but two mispairs, the effect on correct base pairs was much greater than that of mispairs. These results indicate that the hydrogen bond between Arg668 and the minor groove of the primer terminus is important in the fidelity of both formation and extension of mispairs. These experiments support a mechanism in which Arg668 forms a hydrogen bonding fork between the minor groove of the primer terminus and the ring oxygen of the deoxyribose moiety of the incoming dNTP to align the 3′-hydroxyl group with the α-phosphate of the dNTP. This is one mechanism by which the polymerase can use the geometry of the base pairs to modulate the rate of formation and extension of mispairs.

The proficiency of DNA polymerases to incorporate the correct dNTP into DNA is a major factor in the successful replication of DNA. This high fidelity synthesis is accomplished despite the similarity in energy between correctly and incorrectly paired bases (*1*, *2*). Three mechanisms have been proposed to explain how polymerases can achieve a selectivity of 1 in 10 000 with differences in $\Delta G°$ of less than 1 kcal/mol between correct and incorrect base pairs (*3*). (1) Polymerases can amplify the energy difference between correct and incorrect base pairs by excluding water from the active site (*4*). (2) By restricting the movement of the DNA, polymerases can increase the $\Delta\Delta G°$ between the correct and incorrect base pairs (*1*). (3) Polymerases can enhance fidelity by selecting for base pairs of the Watson−Crick geometry (*2*, *5*). These three mechanisms are not mutually exclusive; by providing a check for Watson−Crick geometry, the polymerase would have to restrict the entropy of the DNA thereby increasing the $\Delta G°$ between correct and incorrect base pairs. The geometric selection would probably exclude H_2O from contact with the DNA, thereby increasing $\Delta H°$. All three theories involve interactions between the DNA and polymerase.

Polymerases can select for the correct base pairs based on geometric constraints because the four Watson−Crick base pairs have a similar topography (*6*). Although the general shape of Watson−Crick base pairs are similar, the major groove displays differences for each base pair (*7*). In contrast, the minor groove of the DNA may play an important role in this geometrical selection because the position of two hydrogen bond acceptors ($N3$ of purines and O^2 of pyrimidines) are similar in the four Watson−Crick base pairs but different in mispairs (*7*, *8*). Crystal structures of DNA polymerases bound to DNA have shown that there are many interactions between the protein and the minor groove of DNA (*9*−*13*). Site directed mutagenesis studies have implicated many of these amino acid residues as being important for catalysis and fidelity of DNA replication (*13*−*18*). Similarly, the use of purine analogues such as 3-deazaadenine (*19*, *20*), 3-deazaguanine (3DG[1]) (*21*), 9-methyl-1*H*-imidazo[4,5-*b*]pyridine and 4-methylbenzimidazole (*22*, *23*) and the pyrimidine analogues difluorotoluene (*22*, *23*), 2-aminopyridine and 3-methyl-2-pyridone (*24*) also have implicated the minor groove of the DNA as being crucial to DNA replication.

† Supported by NIH Grant CA 75074.

* To whom correspondence should be addressed at Pennsylvania State University College of Medicine, Department of Biochemistry and Molecular Biology, Room C5709, Mail Code H171, 500 University Drive, Hershey, PA 17033. Phone 717-531-4623, fax 717-531-7072, e-mail tes13@psu.edu.

10.1021/bi047460f CCC: $30.25
Published on Web 03/25/2005

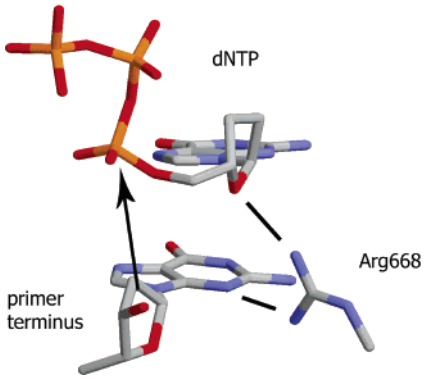

FIGURE 1: Representation of the hydrogen bonding fork between Arg668 and guanine at the 3′-terminus and the deoxyribose ring oxygen of the incoming dGTP. This structure is based upon the ternary crystals of T7 DNA polymerases (*12*) in which the 2′,3′-dideoxyadenosine at the primer terminus was replaced by a 2′-deoxyguanosine using Pymol Ver 0.97 (http://pymol.sourceforge.net/). The picture was created with Rasmol Ver 2.7 (http://www.openrasmol.org/). In the T7 DNA polymerase crystal structure the distance between Arg429 and the *N*3-position of adenine at the primer terminus is 2.86 Å and between Arg429 and the ring oxygen of the incoming 2′,3′-dideoxyguanosine 5′-triphosphate is 2.81 Å.

X-ray crystallographic studies with the closely related BF, *Taq* and T7 DNA polymerases predict a structured minor groove with hydrogen bonds between the minor groove of the DNA and water molecules and amino acid side chains of KF$^-$ (*10*−*12*). These interactions were probed by Morales and Kool and they found that only at the primer terminus did the 9-methyl-1H-imidazo[4,5-*b*]pyridine to 4-methylbenzimidazole substitution result in decreased reaction rates (*23*, *25*).

Utilizing oligodeoxynucleotides containing 3DG, we found evidence that Arg668 makes a critical hydrogen bond to the minor groove of the primer terminus (*26*) as well as to the ring oxygen of the deoxyribose group of the incoming dNTP (*27*). Arg668 can play an essential role in catalysis and fidelity of DNA replication by acting as a fulcrum between the incoming dNTP and primer terminus. When the terminal and nascent base pairs have Watson−Crick geometries then Arg668 can form hydrogen bonds to the minor groove of the primer terminus and the ring oxygen of the incoming dNTP as illustrated in Figure 1. By these interactions Arg668 can align the α-phosphate of the incoming dNTP with the 3′-hydroxyl such that reaction rapidly occurs. With 3DG at the primer terminus, the position of Arg668 is altered such that it cannot correctly align the incoming dNTP and consequently the rate of reaction drops (*26*). In this manuscript, we further examined the interactions between the KF$^-$ minor groove of the DNA to determine whether these interactions are important in fidelity of DNA replication. In addition, we found that the interaction with the primer terminus and the polymerase has a large effect on the fidelity of both formation and extension of mispairs

[1] Abbreviations. 3DG, 3-deazaguanine; 3dDGTP, 2′-deoxy-3-deazaguanosine 5′-*O*-triphosphate; BF, *Bacillus stearothermophilis* DNA polymerase large fragment; BSA, bovine serum albumin; dNTP, 2′-deoxyribose nucleotide 5′-*O*-triphosphate; DTT, dithiothreitol; EDTA, ethylenediamine tetraacetic acid; KF$^+$, Klenow fragment of *E. coli* DNA polymerase I; KF$^-$, Klenow fragment of *E. coli* DNA polymerase I with the proofreading exonuclease inactivated; PAGE, polyacrylamide gel electrophoresis; *Taq*, *Thermus aquaticus*.

EXPERIMENTAL PROCEDURES

General. [^{32}P]ATP was purchased from Amersham at 6000 Ci/mmol. T_4 polynucleotide kinase, and the Klenow fragment of *Escherichia coli* DNA polymerase I with the exonuclease activity inactivated (KF$^-$) were obtained from Promega. The dNTPs (ultrapure grade) were purchased from GE Healthcare, and the concentrations were determined by UV absorbance (*28*). The oligodeoxynucleotides containing 3DG were synthesized, purified by PAGE followed by reverse-phase HPLC, and characterized by enzymatic hydrolysis with HPLC analysis (*21*, *29*). The concentrations of oligodeoxynucleotides were determined from the absorbance at 260 nm, using the method of Borer (*30*) in which it was assumed that the spectroscopic properties of 3DG were identical to G. The primer was ^{32}P-labeled with γ-[^{32}P]ATP in a reaction catalyzed by T_4-polynucleotide kinase. The oligomer was separated from low molecular weight impurities with a spin column (Bio Gel P6) and the primer was annealed with a 50% excess of the template as previously described (*29*). 3′-,5′-Di(*O*-*tert*-butyldimethylsilyl)-2′-deoxy-3-deazaguanosine and 3′-,5′-di(*O*-*tert*-butyldimethylsilyl)-2′-deoxycytidine were prepared from the nucleosides by standard methods (*31*).

Steady-State Kinetics. The polymerase was preincubated in a solution containing the ^{32}P-labeled oligodeoxynucleotide duplex and buffer. The reaction was initiated by the addition of 3 μL dNTP in water to 3 μL DNA-enzyme solution at 37 °C. The composition of the buffer during the reaction was 50 mM Tris-HCl (pH 8.0), 5 mM $MgCl_2$, 5 mM DTT, 100 μg/mL BSA. The concentration of the primer was 100 nM and the template was 150 nM. The KF$^-$ concentrations varied from 0.1 to 10 nM so that the reaction could be conveniently quenched after 5% to 20% of the DNA reacted. The reactions were quenched by the addition of 6 μL of 100 mM EDTA in 95% formamide, containing 0.025% w/v bromophenol blue, and 0.025% w/v xylene cyanol. To determine the k_{cat} and K_m^{dNTP} values, the dNTP concentration was varied from 0 to 1 mM. To determine the K_m^{DNA}, the DNA concentration was varied from 1 to 100 nM while the dNTP concentration was held constant at 150 μM and the KF$^-$ concentration at 0.1 nM.

Pre-Steady-State Kinetics. The reaction was initiated by the addition of 15.9 μL dNTP and $MgCl_2$ in water to 16.4 μL DNA-enzyme solution at 25 °C with a KinTek-3 rapid quench instrument. The composition of the buffer during the reaction was 50 mM Tris-HCl (pH 8.0), 5 mM $MgCl_2$, 5 mM DTT, 100 μg/mL BSA. Typically the DNA concentration was 200 nM and the polymerase concentration was 100 nM. The concentration of dNTPs varied from 0 to 500 μM. The reactions were quenched by the addition of 300 mM EDTA.

Product Analysis by PAGE. The progress of the reaction was analyzed by denaturing PAGE in 20% acrylamide (19:1, acrylamide-*N*,*N*′-methylene bisacrylamide), 7 M urea in 1× TBE buffer (0.089 M Tris, 0.089 M boric acid, 0.002 M Na_2EDTA). The size of the gel was 40 × 33 × 0.4 cm and was run at 2000 V for 2−2.5 h. The radioactivity on the gel was visualized with a Bio Rad GS 250 Molecular Imager. The progress of the reaction was quantitated by dividing the total radioactivity in the product band(s) by the radioactivity in the product and reactant bands. Multiple product bands

appeared when the incorrect dNTP was added to the reaction.

Data Analysis. Data were fitted by nonlinear regression using the program Prism version 4 for Windows (GraphPad Software, San Diego California USA, www.graphpad.com). Data from the steady-state reactions were fitted to eq 1 in

$$v_0 = k_{cat}[E]_0[dNTP]_0/([dNTP]_0 + K_m) \quad (1)$$

which v_0 is the initial rate, k_{cat} is the maximum rate of dNTP incorporation, E is the KF^-, and K_m is the Michaelis constant for either the dNTP or DNA depending on which was varied. Data from the burst equations were fitted to eq 2, where P

$$P = A(1 - e^{-kt}) + k_{ss}t \quad (2)$$

is the product formed, A is the burst amplitude, which corresponds to the concentration of the enzyme in the active form, k is the first-order rate for the dNTP incorporation, and k_{ss} is the observed steady-state rate constant. When a burst was not observed, the data were fit to eq 3, where P is

$$P = A(1 - e^{-kt}) \quad (3)$$

the product formed, A is the total amount of DNA reacted, and k is the first-order rate for the dNTP incorporation. The k values for these experiments were fitted to eq 4, where

$$k = k_{pol}[dNTP]/([dNTP] + K_d) \quad (4)$$

k_{pol} is the maximum rate of dNTP incorporation and K_d^{dNTP} is the equilibrium dissociation constant for the interaction of dNTP with the polymerase-DNA complex. The K_d^{DNA} was determined from eq 5 in which the burst amplitude (A)

$$A = \frac{[DNA]_0 + K_d^{DNA} + [E]_0 - \sqrt{([DNA]_0 + K_d^{DNA} + [E]_0)^2 - 4[DNA]_0[E]_0}}{2} \quad (5)$$

was determined at various DNA concentrations at a constant polymerase concentration ([E]).

pK_a of 2′-Deoxy-3-deazaguanine. The pK_a's of 2′-deoxy-3-deazaguanine were determined spectrophotometrically, by measuring the UV spectra at various pH values. The solutions were buffered with 50 mM phosphate (pH 1 to 2.5, 7 to 8, and 11.5 to 13.5), citrate (pH 3 to 6), and glycine (pH 9−11). The pK_a values were determined by fitting absorbance versus pH with eq 6, in which A_{low}, A_{high}, and A_{pH} are the

$$A_{pH} = A_{low} + \frac{A_{high} - A_{low}}{1 + 10^{pK_a - pH}} \quad (6)$$

absorbances at a low, high, and specific pH values at 310 and 326 nm.

Base Pair Formation between Cytosine and 3DG. Hydrogen bonding between 3′,5′-di(*O-tert*-butyldimethylsilyl)-2′-deoxy-3-deazaguanosine and 3′,5′-di(*O-tert*-butyldimethylsilyl)-2′-deoxycytidine (*31*). in $CDCl_3$ (99.8% D, Cambridge Isotope Lab., Andover MA) was evaluated by ^{1}H NMR spectroscopy. The ^{1}H NMR spectra were obtained with a 360 MHz Bruker Model AM 360 Wide Bore NMR. Typically, 64 transients were accumulated over 5400 Hz using a 90° pulse and a 2 s relaxation delay. Chemical shifts

Scheme 1: Differences in pK_a's and Hydrogen Bonding Potential between Guanine and 3-Deazaguanine

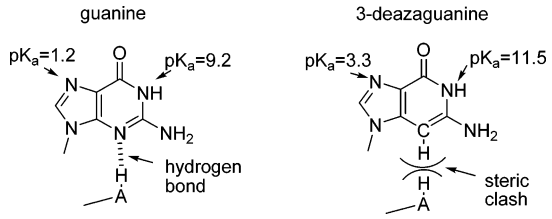

are in reference to TMS. The temperature was not controlled and was approximately 22 °C. The total nucleoside concentration was 20 mM with various ratios of C to 3DG. Nucleoside concentrations were determined by mass and relative nucleotide concentrations were reconfirmed by NMR integrated peak intensities.

UV Spectroscopy and Thermal Denaturation Studies. Samples (325 μL) for thermal denaturation studies contained an equimolar ratio of 5′-CAG ACG ACG-3′ and 5′-CGT CGT CTX-3′ (X is G or 3DG) in 50 mM cacodylic acid-NaOH (pH 7.0), 1 M NaCl, 1 mM EDTA. The UV spectra and absorbance measurements were recorded on a Beckman DU640 UV−vis spectrophotometer equipped with a 6 × 325 μL cuvette Peltier temperature controller. Absorbances were monitored at 260 nm while the temperature was varied; specifically, following a 10 min incubation period at 20 °C the temperature was ramped (1 °C per min) up to 85 °C and back down to 20 °C over a 140 min period. The collected data were then normalized to the fraction of single-stranded DNA (f), through the equation: $f = (A - A_{DS})/(A_{SS} - A_{DS})$, where A is the absorbance of sample at a particular temperature, A_{SS} is the average single-stranded absorbance, and A_{DS} is the average double-stranded absorbance. The T_m was the temperature at which $f = 0.5$. Each T_m is the average of three separate experiments. The thermodynamic parameters were determined by fitting T_m versus C_T according to eq 7 by nonlinear regression.

$$\frac{1}{T_m} = \frac{R}{\Delta H^\circ}\ln\left(\frac{C_T}{4}\right) + \frac{\Delta S^\circ}{\Delta H^\circ} \quad (7)$$

RESULTS

Use of 3DG To Probe Interactions with 3-Position of Guanine. We have used the G to 3DG substitution to probe functional interactions between the polymerase and the 3-position of guanine at various positions in the polymerase binding site. As illustrated in Scheme 1, the carbon for nitrogen substitution eliminates the possibility of a hydrogen bond to the 3-position of guanine while the overall geometry and Watson−Crick and Hoogsteen hydrogen bonding sites remain unchanged. Our premise is that a decrease in rate resulting from the G to 3DG substitution is caused by a disruption of a critical interaction between the polymerase and the 3-position of guanine. For this premise to be correct, the physical properties of G and 3DG should be very similar, except at the 3-position. Therefore we examined several physical properties of 3DG including its pK_a's, the ability of 3DG to hydrogen bond with cytosine, and the thermodynamics of 3DG in a DNA duplex.

Base Pair Formation between Cytosine and 3DG. Potential hydrogen bond interactions between 3DG and C were

Table 1: Thermodynamic Parameters for the Thermal Denaturation of Guanine or 3-Deazaguanine in the Center or 3′-End of a DNA Duplex

5′- C G T C **X** T C T **Y** -3′
3′- G C A G C A G A C -5′

X	Y	ΔH° (kcal/mol)	ΔS° (cal/(mol·K))	ΔG° at 298 K (kcal/mol)
G	G	−87 ± 7	−270 ± 20	−6.1 ± 0.5
3DG	G	−72 ± 11	−230 ± 50	−3.5 ± 0.1
G	3DG	−82 ± 8	−260 ± 25	−5.0 ± 0.5

investigated using ^{1}H NMR spectroscopy. NMR experiments in nonaqueous solvents have shown that adenine pairs with uracil and guanosine with cytidine (*32*). Except for a weak self-interaction with guanosine, no other hydrogen bonding interactions were found (*32*). In other experiments, it was found that O^6-methylguanine forms hydrogen bonds with thymine but only with cytosine when protonated (*33*). These two experiments suggest that random hydrogen bonds are not observed by this technique and that only a complex held together by at least two hydrogen bonds is observed. The 3′- and 5′-hydroxy groups of 2′-deoxy-3-deazaguanosine and 2′-deoxycytidine were protected with the *tert*-butyldimethylsilyl moieties to make the 2′-deoxynucleosides soluble in $CDCl_3$ (*31*). The spectra were measured at various ratios of 3DG to C at a constant total nucleoside concentration of 20 mM. The chemical shifts of the *N*1 and *N*2-protons of 3DG increased as the mole fraction of cytidine was increased (Supplementary data Figure S1A and B). Similarly, as the amount of 3DG was increased, the chemical shift of the *N*4-proton of cytidine increased (Figure S1C). The increases in chemical shifts are consistent with the formation of hydrogen bonds. Thus, our results strongly suggest that 3DG forms Watson−Crick base pair with cytosine in $CDCl_3$. Consequently, it should be formed in DNA as well.

UV Thermal Denaturation Studies. The stability of 3DG in DNA was evaluated by thermal denaturation studies of oligodeoxynucleotide duplexes (illustrated in Table 1) containing G or 3DG in the center or 3′-end of one strand (Figure S2A). The T_m values were determined by the mean of six experiments. Incorporation of 3DG in the center of the duplex decreased the T_m more than when placed at the 3′-terminus. The thermodynamic parameters listed in Table 1 were determined by fitting T_m versus C_T according to eq 7 with nonlinear regression (Figure S2B). The duplex was destabilized by 2.5 kcal/mol when 3DG was placed at the center but only by 1 kcal/mol when placed at the 3′-terminus. These results indicate that 3DG destabilizes the DNA helix.

pK_a of 2′-Deoxy-3-deazaguanine. The UV spectrum of 2′-deoxy-3-deazaguanine is dependent on pH (Figure S3A). As the pH is lowered from 7 to 1, the maxima at 269 and 299 shift to 282 and 315 nm. This change produces a pK_a of 3.3 when fitted to a sigmoidal equation (Figure S3B). As the pH is changed from 7 to 14, the maxima at 269 and 299 nm are converted a single maximum at 277 nm. This change is dependent on a pK_a of 11.5 when fitted to a sigmoidal equation. By comparison with guanine, we assigned the pK_a of 3.3 to the N7 position and the pK_a of 11.5 to the N1-position. Thus, 3DG is neutral at physiological pH, but is more basic than guanine, which has pK_a's of 1.2 and 9.2 (*34*).

The increased bascity may result in weaker hydrogen bonds with the opposite cytosine because hydrogen bonds are stronger when the pK_a's of the participants are similar (*35*, *36*). Since the pK_a of the N3 of deoxycytidine is 4.1 (*34*), the change of the pK_a on guanine from 9.2 (*34*) to 11.5 should decrease the strength of the hydrogen bond between the bases. As a result, this effect may be in part the reason 3DG is a slightly poorer substrate than G. However, despite the increased basicity of 3DG, it remains neutral at physiological pH and should be able to participate in Watson−Crick hydrogen bonding with cytosine.

Kinetics of Incorporation of a Single Base Pair. The catalytic importance of interactions between the polymerase and the minor groove of DNA was investigated by comparing the rates of incorporation of a single nucleotide with G or

Scheme 2: Oligodeoxynucleotides Used in This Study To Examine the Minor Groove Interactions in the Active Site

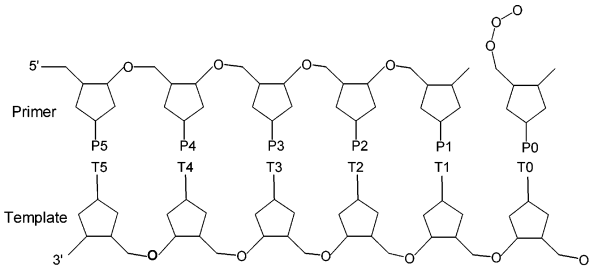

P0 5′-GCACCGCAGACGCA -3′
3′-CGTGGCGTCTGCGTCGTCAGCGTC-5′

T0(X) 5′-GCACCGCAGACGCAG -3′
3′-CGTGGCGTCTGCGTC**X**TCAGCGTC-5′

P1(X) 5′-GCACCGCAGACGCA**X** -3′
3′-CGTGGCGTCTGCGTCGTCAGCGTC-5′

T1(X) 5′-GCACCGCAGACGCAGC -3′
3′-CGTGGCGTCTGCGTC**X**TCAGCGTC-5′

P2(X) 5′-GCACCGCAGACGCA**X**C -3′
3′-CGTGGCGTCTGCGTCGTCAGCGTC-5′

T2(X) 5′-GCACCGCAGACGCAGCA -3′
3′-CGTGGCGTCTGCGTC**X**TCAGCGTC-5′

P3(X) 5′-GCACCGCAGACGCA**X**CA -3′
3′-CGTGGCGTCTGCGTCGTCAGCGTC-5′

T3(X) 5′-GCACCGCAGACGCAGCAG -3′
3′-CGTGGCGTCTGCGTC**X**TCAGCGTC-5′

P4(X) 5′-GCACCGCAGACGCA**X**CAG -3′
3′-CGTGGCGTCTGCGTCGTCAGCGTC-5′

T4(X) 5′-GCACCGCAGACGCAGCAGT -3′
3′-CGTGGCGTCTGCGTC**X**TCAGCGTC-5′

P5(X) 5′-GCACCGCAGACGCA**X**CAGT -3′
3′-CGTGGCGTCTGCGTCGTCAGCGTC-5′

T5(X) 5′-GCACCGCAGACGCAGCAGTC -3′
3′-CGTGGCGTCTGCGTC**X**TCAGCGTC-5′

Table 2: Kinetic Parameters for the Incorporation of a Single dNTP into an Oligodeoxynucleotide Duplex with G or 3DG at Different Positions[a]

substrate	X	dNTP	template	k_{cat}/K_m[b] ($s^{-1}\ \mu M^{-1}$)	k_{pol}[c] (s^{-1})	K_d^{dNTP}[c] (μM)	k_{pol}/K_d^{dNTP}[c] ($s^{-1}\ \mu M^{-1}$)
P0		dGTP	C	2.6 ± 0.50	310 ± 80	10 ± 5	31 ± 17
P0		d3DGTP	C	0.27 ± 0.07	50 ± 20	20 ± 10	2.5 ± 1.5
P1	G	dCTP	G	0.97 ± 0.20	155 ± 20	22 ± 7	7 ± 2
P1	3DG	dCTP	G	0.0033 ± 0.003	0.38 ± 0.08	30 ± 11	0.013 ± 0.005
P2	G	dATP	T	0.83 ± 0.33	590 ± 140	10 ± 2	59 ± 18
P2	3DG	dATP	T	0.17 ± 0.05	350 ± 20	3.3 ± 0.6	106 ± 20
P3	G	dGTP	C	0.63 ± 0.12	440 ± 20	8 ± 2	55 ± 14
P3	3DG	dGTP	C	0.88 ± 0.13	360 ± 20	9 ± 2	40 ± 9
P4	G	dTTP	A	0.55 ± 0.15	400 ± 100	10 ± 3	40 ± 16
P4	3DG	dTTP	A	1.8 ± 0.5	200 ± 20	15 ± 3	13 ± 3
P5	G	dCTP	G	*d*	520 ± 70	26 ± 10	20 ± 8
P5	3DG	dCTP	G	*d*	600 ± 140	17 ± 11	35 ± 24
T0	G	dCTP	G	0.97 ± 0.20	155 ± 20	22 ± 7	7 ± 2
T0	3DG	dCTP	3DG	0.47 ± 0.23	106 ± 12	20 ± 9	5.3 ± 2.5
T1	G	dATP	T	0.83 ± 0.33	590 ± 140	10 ± 2	59 ± 18
T1	3DG	dATP	T	2.5 ± 0.8	200 ± 20	10 ± 1	20 ± 3
T2	G	dGTP	C	0.63 ± 0.12	440 ± 20	8 ± 2	55 ± 14
T2	3DG	dGTP	C	0.28 ± 0.05	63 ± 5	3 ± 1	21 ± 7
T3	G	dTTP	A	0.55 ± 0.15	400 ± 100	10 ± 3	40 ± 16
T3	3DG	dTTP	A	0.25 ± 0.10	130 ± 30	15 ± 5	8 ± 4
T4	G	dCTP	G	1.8 ± 0.5	520 ± 70	26 ± 10	20 ± 8
T4	3DG	dCTP	G	1.5 ± 0.3	900 ± 160	50 ± 20	18 ± 7
T5	G	dATP	T	0.98 ± 0.25	330 ± 30	16 ± 4	21 ± 5
T5	3DG	dATP	T	0.922 ± 0.23	136 ± 20	3 ± 2	45 ± 30

[a] See Scheme 1 for sequences of oligodeoxynucleotides. The kinetic parameters were determined from the fitting of eqs 1 and 4. The errors are the standard errors from the nonlinear regression. Typically, seven to ten concentrations of dNTP were used to obtain these values. [b] Carried out by the addition of the dNTP to a premixed solution containing buffer, DNA, and polymerase. The final buffer conditions were 50 mM Tris-HCl (pH 8.0), 5 mM $MgCl_2$, 5 mM DTT, and 100 μg/mL BSA at 37 °C. The concentration of the primer was 100 nM, and that of template was 150 nM. The KF^- concentrations varied from 0.01 to 10 nM. The k_{cat} and K_m values were determined from eq 1 from at least seven concentrations of dNTP that were determined in triplicate. [c] Carried out by the addition of the dNTP to a premixed solution containing buffer, DNA, and polymerase. The buffer during the reaction was 50 mM Tris-HCl (pH 8.0), 5 mM $MgCl_2$, 5 mM DTT, and 100 μg/mL BSA at 25 °C. The concentration of the DNA (200 nM) was in excess over the polymerase (100 nM). The burst rate constant (k) was determined from time courses with at least 10 time points in duplicate. k_{pol} and K_d^{dNTP} were determined with eq 4 with at least seven concentrations of dNTP. [d] Not determined.

3DG at different positions in the binding pocket, as illustrated in Scheme 2. The steady-state kinetic analyses were carried out with 10- to 1000-fold excess of the DNA (100 nM) over the polymerase (0.1 to 10 nM). The initial rates were based upon a single time point. The concentration of KF^- was varied to have initial rate time points between 1 and 30 min. The k_{cat}/K_m values for the incorporation of the correct dNTP into the oligodeoxynucleotides containing G ranged from 0.55 to 2.6 $s^{-1}\ \mu M^{-1}$ as reported in Table 2.

The pre-steady-state analyses were initiated by the mixing of a buffered polymerase − DNA solution to the dNTP and $MgCl_2$ in H_2O. When the DNA was in excess over the polymerase, the incorporation of the correct dNTP exhibited a burst of product formation that was followed by a slower increase in product formation. The burst was due to the formation of product from the preformed polymerase−DNA complex. The rate-limiting step of this phase had been determined to be the conformational change preceding phosphodiester bond formation in step 4 in Scheme 3 (*37*−*39*). The subsequent slower increase in product formation was limited by the dissociation of the polymerase from the DNA. The k_{pol} varied from 155 to 590 s^{-1} and the K_d^{dNTP} varied from 8 to 29 μM (Table 2).

*G to 3DG Substitution on Incoming dNTP (**P0**).* The importance of hydrogen bonds from the polymerase to the minor groove of the dNTP was evaluated by comparing the incorporation of dGTP and d3DGTP opposite C using **P0**. The steady-state kinetics showed that d3DGTP was incorporated opposite C with a 10-fold lower k_{cat}/K_m than dGTP,

Scheme 3: Minimal Kinetic Scheme for Replication of DNA by the Klenow Fragment of DNA Polymerase I of *E. coli*

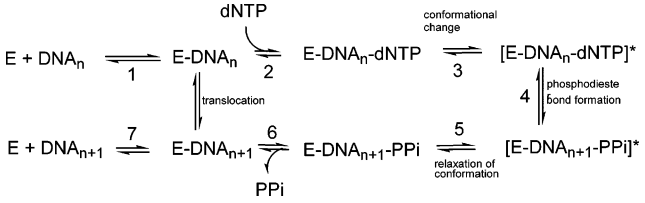

that was primarily due to an increase in K_m. Under pre-steady-state conditions, the incorporation of d3DGTP followed burst kinetics as illustrated in Figure 2A. The burst amplitude was not affected by the G to 3DG substitution and was approximately equal to the polymerase concentration. As illustrated in Figure 2B, the k_{pol} decreased 6-fold (310 to 50 s^{-1}) while the K_d^{dNTP} increased 2-fold (10 to 20 μM) to produce a 14-fold decrease in k_{pol}/K_d.

*G to 3DG Substitution at the Template Position (**T0**).* Substitution of 3DG for G at **T0** produced only a 2-fold decrease in k_{cat}/K_m. Under pre-steady-state conditions, incorporation of dCTP opposite G as well as 3DG followed burst kinetics. The G to 3DG substitution did not greatly affect the kinetic parameters, k_{pol} decreased from 155 to 106 s^{-1} while K_d^{dNTP} decreased from 29 to 20 μM. In these reactions, the burst amplitude is the concentration of E-DNA_n that is in the correct conformation to bind and then react with the dNTP. Dissociation constants of DNA to polymerases (K_d^{DNA}) have been determined by measuring the

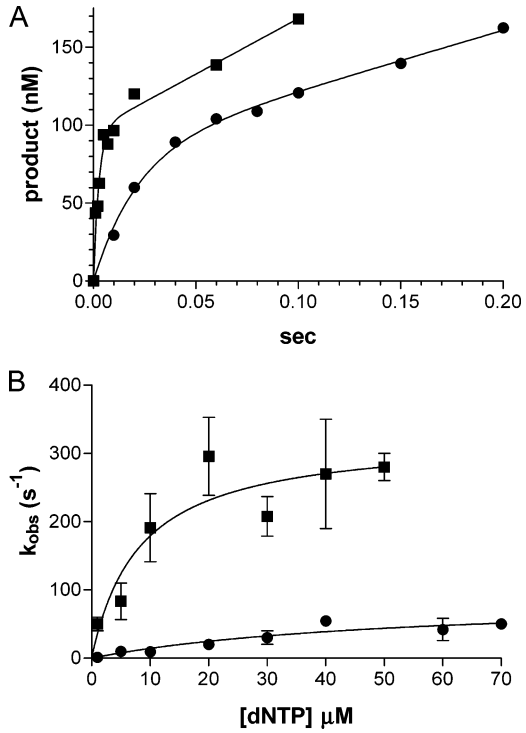

FIGURE 2: Incorporation of dGTP (■) and d3DGTP(●) opposite C with a KF^- concentration of 25 nM and a P0(G) concentration of 100 nM. Panel A shows the time course of incorporation of dNTP opposite C fitted to burst eq 2. Panel B show the plot of *k* versus [dNTP]. The solid line shows the best-fit of the data to eq 4.

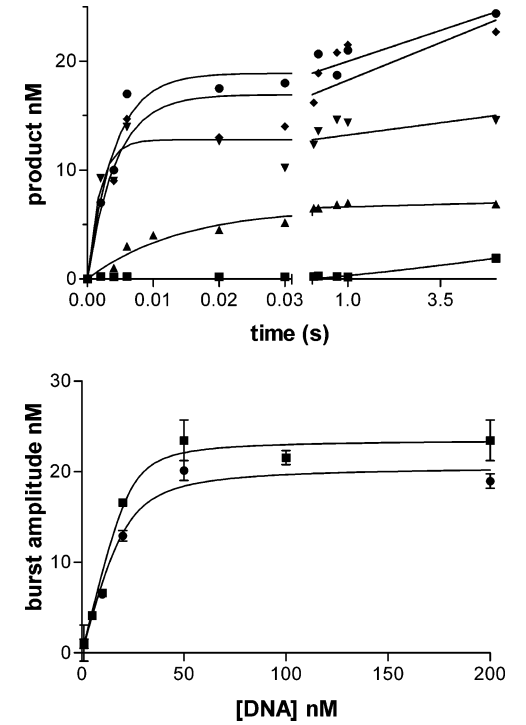

FIGURE 3: Determination of K_d^{DNA} for **T0(3DG)**. A. Time course of incorporation of dCTP (150 μM) opposite 3DG with 20 nM KF^- and 1 (■), 10 (▲), 20(▼), 50 (◆), and 200 (●) nM **T0(3DG)**. The lines are the data fitted to eq 2. B. Plot of the burst amplitude versus DNA concentration for **T0(G)** (■) and **T0(3DG)** (●). The solid lines are the best-fit of the data to eq 5.

burst amplitude at different concentrations of DNA (*40*). Figure 3 shows the increasing burst amplitudes of the incorporation of dCTP into **T0(3DG)** with increasing DNA concentrations. The burst amplitudes were plotted against the DNA concentration and the K_d^{DNA} values were determined by fitting the burst amplitudes to the DNA concentration with eq 5 (Figure 3B). We found that the binding to the DNA was unaffected by the G to 3DG substitution at **T0** (Table 3).

Table 3: Effect of G to 3DG Substitution of the Binding of DNA to Polymerase

substrate	G	3DG
T0(X)[a]	1.5 ± 0.5	1.6 ± 0.5
T1(X)[a]	1.9 ± 0.9	10 ± 4
T2(X)[a]	5 ± 4.0	4 ± 1
P1(X)[b]	1.5 ± 0.8	6.5 ± 1.5
P2(X)[a]	1.9 ± 0.9	0.9 ± 0.4
P3(X)[a]	5 ± 4	3.9 ± 0.9

[a] K_d^{DNA} (nM) was determined by analyzing the burst amplitude of the reaction between 20 nM KF^- and seven to ten concentrations of DNA with eq 5. The burst amplitudes were determined from eq 2 with at least 12 time points. [b] K_d^{DNA} (nM) was determined by analyzing the first-order rate constants of the reaction between 25 nM DNA and seven concentrations of KF^- with eq 5.

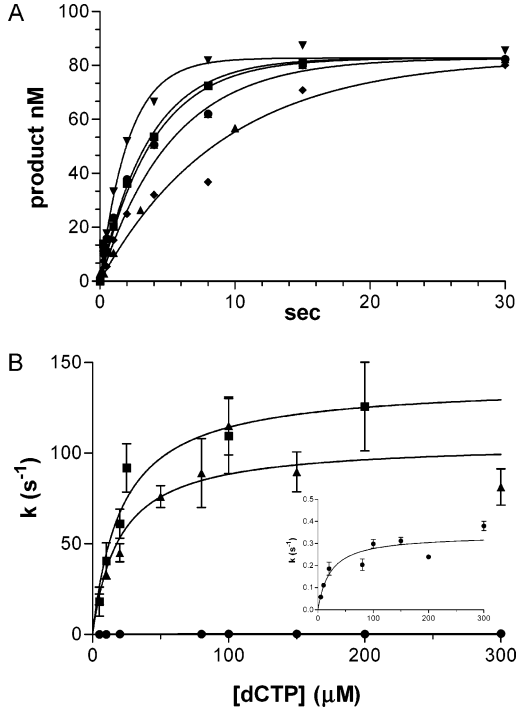

FIGURE 4: DNA replication with **P1(X)** and **T0(X)**. A. Time course for the incorporation of dCTP opposite dG with 3DG at the primer terminus (**P1(3DG)**). The concentration of KF^- was 100 nM and DNA was 200 nM. The concentration of dCTP was 5 (◆), 25 (▲), 50 (●), 100 (■), 300 (▼) μM. The lines are the nonlinear least-squares fit of the data to eq 2. B. Plot of k_{obs} vs dCTP with **P1(G)** and **T0(G)** (■), **T0(3DG)** (▲) and **P1(3DG)** (●). The solid lines are the best fit to eq 4.

*G to 3DG Substitution at the Primer Terminus, **P1**.* Incorporation of 3DG at the primer terminus decreased the k_{cat}/K_m approximately 300-fold through a decrease in k_{cat}. The pre-steady-state time courses did not exhibit burst kinetics but were consistent with first-order kinetics (eq 3) as illustrated in Figure 4A. With a polymerase concentration of 50 nM and a DNA concentration of 100 nM, the average amplitude for the extension past 3DG was 83 ± 10 nM, indicating that approximately 83% of the DNA reacted. The rate of reaction was dependent on dCTP concentration; the

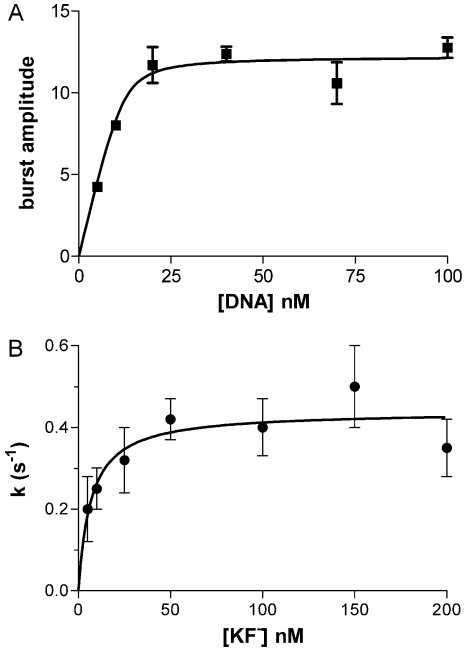

FIGURE 5: $K_d^{DNA}$with guanine or 3-deazaguanine at primer terminus. A. Plot of the burst amplitude versus DNA concentration for **P1(G)** with a KF$^-$ concentration of 12.5 nM and dCTP concentration of 150 μM. B. Plot of k_{obs} versus polymerase concentration with 50 nM DNA and 150 μM dCTP. The solid lines are the best fit of the data to eq 5 in which *A* is the burst amplitude (A) or first-order rate constant (B).

comparison between **P1(G)** and **P1(3DG)** is illustrated in Figure 4B. The burst or first-order rate constants were fitted to eq 4 to obtain k_{pol} and K_d^{dNTP} values. The rate of extension past 3DG was reduced approximately 400-fold due to a decreased k_{pol}. (from 155 to 0.38 s^{-1}) without affecting the K_d^{dNTP} which increased only slightly from 22 to 30 μM.

The reduction in k_{pol} can potentially be due to decreased binding of **P1(3DG)** to the polymerase. The K_d^{DNA} for **P1-(G)** was determined by fitting the burst amplitude to eq 5. As illustrated in Figure 5A, the K_d^{DNA} was approximately 1.5 nM. This method, however, cannot be used to determine the K_d^{DNA} for **P1(3DG)** because this reaction did not exhibit burst kinetics, but exhibited first-order kinetics. We therefore examined the binding of enzyme to substrate in the reverse manner by measuring the rate of reaction of **P1(3DG)** with various concentrations of KF$^-$. The results, plotted in Figure 5B, illustrate that the rate of incorporation initially increased and then leveled off as the [KF$^-$] increased. The rate constant for the extension past 3DG was dependent on polymerase concentration when [KF$^-$] < [DNA]. But when [KF$^-$] > [DNA], k_{obs} was independent of [KF$^-$]. The k_{obs} was fitted to eq 5, with A as the k_{obs}, to obtain a K_d^{DNA} of 6.5 nM. This value was increased 4-fold from 1.5 nM obtained with **P1-(G)**. The maximal k_{pol} value obtained in these experiments of 0.4 s^{-1} is approximately equal to the k_{pol} of 0.38 s^{-1} obtained from the experiment in which the dNTP concentration was varied (Figure 4). These results indicate that the G to 3DG substitution at the primer terminus does not appreciably affect the binding of the substrate to enzyme and therefore reduction in k_{pol} is not a result of decreased binding of **P1(3DG)** to KF$^-$.

Summary of Minor Groove Interactions. The k_{pol} and K_d^{dNTP} values for the substrates **P2(X)**-**P5(X)** and **T1(X)**-

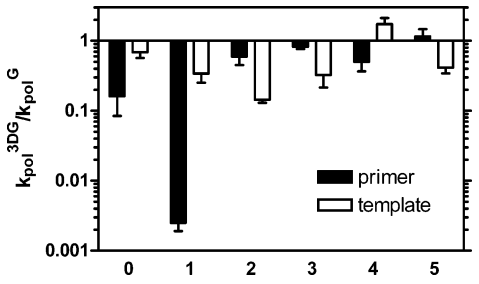

FIGURE 6: Change in k_{pol} due to the G to 3DG substitution, at various positions in the primer (■) and template (□). The *Y*-axis is the ratio of the k_{pol} with 3DG in the DNA to that with G in the DNA. A bar pointing downward would indicate a decreased k_{pol} as a result of the G to 3DG substitution.

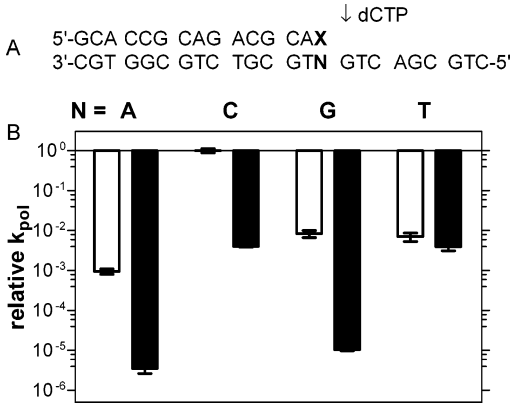

FIGURE 7: Influence of the minor groove primer terminus on mispair extensions. A. Oligodeoxynucleotides used in these reactions in which X = G (□) or 3DG (■). The reactions were carried out as described in the Experimental Procedures with 100 nM KF$^-$ and 25 nM DNA. B. The relative k_{pol} are plotted for the various substrates. The downward direction indicates that the k_{pol} is less than that for standard reaction in which X = G and N = C.

T5(X) were determined as described above and it was found that only minimal differences existed between the G and 3DG substrates. Figure 6 shows a summary of the effect that the G to 3DG substitution had on k_{pol} at the various positions in the binding site. The largest decrease was observed at the primer terminus (P1) in which a 400-fold reduction in k_{pol} was observed. The next largest rate reduction was observed at the incoming dNTP (P0), in which the G to 3DG substitution decreased k_{pol} 6-fold and increased K_d^{dNTP} 2-fold. Small decreases in k_{pol} and increases in K_d^{dNTP} (less than 10-fold) were observed with the G to 3DG substitution at all other positions.

The binding of the DNA to the polymerase was examined with **T0(X)**, **T1(X)**, **T2(X)**, **P2(X)**, and **P3(X)** as described above for **P1(G)** and the results are presented in Table 3. The K_d^{DNA} varied the greatest at T1, in which the G to 3DG substitution increased the K_d^{DNA} 5-fold from 1.9 nM to 10 nM. In all other positions the difference in K_d^{DNA} varied minimally.

Mispair Extension. Since KF$^-$ extends mispairs more slowly than correct base pairs, we examined whether the hydrogen bond between Arg668 and the N3-guanine at the primer terminus is important in the ability of the polymerase to select against extension of mispairs. To this end, we reacted KF$^-$ with the oligodeoxynucleotides presented in Figure 7A in which G and 3DG at the primer terminus were paired against all four bases. In these reactions we incubated

Table 4: Kinetic Parameters for the Extension of X/N Base Pairs[a]

5′- GCACCGCAGACGCA**X** -3′

3′- CGTGGCGTCTGCGT**N**GTCAGCGTC-5′

N	X	k_{pol} (s^{-1})	K_d^{dNTP} (μM)
A	G	0.052 ± 0.008	16 ± 9
A	3DG	0.00020 ± 0.00005	10 ± 7
C	G	55 ± 7	6 ± 3
C	3DG	0.22 ± 0.01	76 ± 19
G	G	0.46 ± 0.09	20 ± 14
G	3DG	0.00057 ± 0.00003	34 ± 9
T	G	0.39 ± 0.09	107 ± 56
T	3DG	0.22 ± 0.05	79 ± 40

[a] The reactions were initiated by the addition of the dCTP and $MgCl_2$ to a premixed solution containing buffer, DNA, and polymerase. The buffer during the reaction was 50 mM Tris-HCl (pH 8.0), 5 mM $MgCl_2$, 5 mM DTT, and 100 μg/mL BSA at 25 °C. The concentration of the KF^- (100 nM) was in excess over the DNA (25 nM). The first-order rate constants were determined from time courses with at least five time points in duplicate. k_{pol} and K_d^{dNTP} were determined with eq 4 with at least seven concentrations of dNTP.

DNA (25 nM) with an excess of KF^- (100 nM) with varying concentrations of dCTP. The first-order rate constants obtained from the time course experiments (eq 1) were plotted against [dCTP] to obtain k_{pol} and K_d^{dNTP} according to eq 2. The parameters are reported in Table 4.

The changes in k_{pol} relative to the extension of the G/C base pair are shown in Figure 7B. The clear bars show the parameters for X = G. As is illustrated by the downward bars with N = A, G and T, the extension past mispairs was slower than extension of the correct (G/C) base pair. The decreases in k_{pol}/K_d^{dNTP} of approximately 1000 were primarily due to decreases in k_{pol}, in conjunction with 2.5 to 6-fold increases in K_d^{dNTP}. The black bars show the changes in k_{pol} due to the G to 3DG substitution at the primer terminus. The four pairs of bars show the effect of the G to 3DG substitution on the extension reaction. For N = A, C, and G, the G to 3DG substitution caused a decrease in k_{pol}. In contrast, with N = T, the G to 3DG substitution did not result in a reduced k_{pol} (Figure 7B). Additionally, the G to 3DG substitution induced a 10-fold increase in K_d^{dNTP} only in the extension past the correct G/C base pair (Table 4). The substitution did not affect K_d^{dNTP} for extension past mispairs. Thus, the hydrogen bond to the N3-position of guanine at the primer terminus occurs and is important during the extension past G/C, G/A, and G/G mispairs but not G/T mispairs. These results also lead to the conclusion that the loss of the minor groove hydrogen bond may be a mechanism by which KF^- selects against extension of the G/T mispair.

Fidelity of Mispair Formation. The influence of the hydrogen bond between Arg668 and the 3-position of guanine at the primer terminus was examined with the oligodeoxynucleotides in Figure 8A. The DNA duplexes are the same except for the primer terminus, which is G or 3DG, and the template base, which is A, C, G, or T. In these reactions we incubated DNA (25 nM) with an excess of KF^- (100 nM) with varying concentrations of dNTP. The first-order rate constants obtained from the time course experiments (eq 1) were plotted against [dCTP] to obtain k_{pol} and K_d^{dNTP} according to eq 4. With 3DG at the primer terminus, the reaction went to 80 to 90% completion when the correct base pair was formed. However, with the incorrect dNTP,

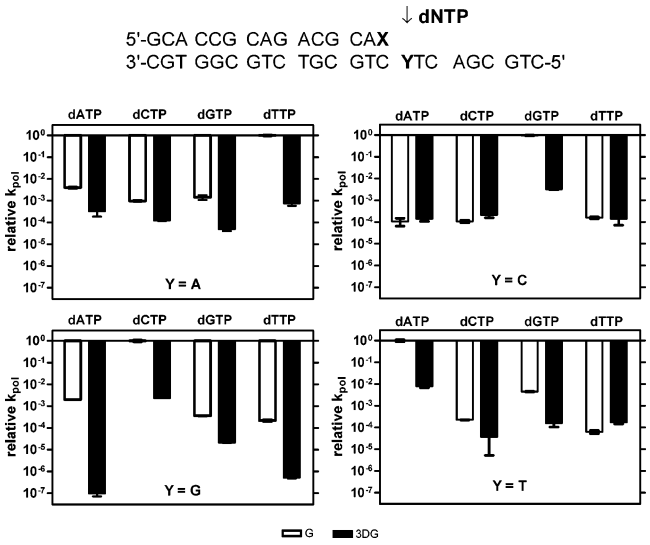

FIGURE 8: Influence of the minor groove primer terminus on mispair formation. A. Oligodeoxynucleotides used in these reactions in which X = G (□) or 3DG (■). The reactions were carried out as described in the Experimental Procedures with 100 nM KF^- and 25 nM DNA. The bar graph shows the k_{pol} relative to that with X = G and the correct base pair incorporation. Panel B shows the data with Y = A, panel C with Y = C, panel D with Y = G, and panel E with Y = T.

the reactions proceeded to approximately 60% completion over the 60 min incubation period. This result may be a consequence of the denaturation and inactivation of the polymerase over the incubation period or the formation of an inactive polymerase-DNA complex. The parameters are reported in Table 5 and the relative k_{pol} values are plotted in Figure 8. The open bars represent the relative k_{pol} with X = G while the black bars represent the relative k_{pol} with X = 3DG. The data show that KF^- incorporated the correct dNTP with approximately 30,000-fold more efficiently than the incorrect dNTP. The selectivity is primarily due to a decreased k_{pol}, although the K_d^{dNTP} is also increased approximately 10-fold for mispair formation.

With A as the template base and X = G, mispair formation was 16 000- to 48 000-fold less efficient primarily due to a decrease in k_{pol} (Table 5). The G to 3DG-substitution induced a 1300-fold decrease in k_{pol} with the correct dTTP but only a 10- to 30-fold decrease during mispair formation (Y = A, Figure 8B). The K_d^{dNTP} was not affected by the substitution. These results suggest that the Arg668-N3-guanine hydrogen bond occurs during correct base pair formation but is less strong or not present during mispair formation.

With C as the template base (Figure 8C), the selectivity against mispair formation was based almost entirely on differences in k_{pol}. The G to 3DG substitution induced a 300-fold decrease in k_{pol} with a 3.5-fold increase in K_d^{dNTP} for dGTP while the G to 3DG substitution did not affect the rate of mis-incorporation of dCTP. Incorporation of dATP and dTTP opposite C exhibited substrate inhibition; at dNTP concentrations over 50 μM, the rate of reaction decreased. Thus, in Table 5 and Figure 8C, the k_{pol} number is the maximal first-order rate constant obtained in the reaction. Thus, the true k_{pol} and K_d^{dNTP} values may be higher than those used in Table 5 and Figure 8C. Therefore, the G to 3DG substitution do not result in a decrease in k_{pol} for the incorporation of dATP and dTTP opposite C. These results

Table 5. Kinetic Parameters for the Formation of Mispairs with G or 3DG at the Primer Terminus[a]

5′- GCACCGCAGACGCA**X** -3′
3′- CGTGGCGTCTGCGTC**Y**TCAGCGTC-5′

dNTP	Y	X	k_{pol} (s^{-1})	K_d^{dNTP} (μM)
dATP	A	G	0.45 ± 0.05	270 ± 80
dATP	A	3DG	0.037 ± 0.016	126 ± 209
dCTP	A	G	0.11 ± 0.01	196 ± 67
dCTP	A	3DG	0.014 ± 0.001	200 ± 4
dGTP	A	G	0.16 ± 0.04	230 ± 100
dGTP	A	3DG	0.0055 ± 0.001	30 ± 20
dTTP	A	G	113 ± 10	4 ± 1
dTTP	A	3DG	0.086 ± 0.021	16 ± 14
dATP	C	G	0.015 ± 0.006	22 ± 3
dATP	C	3DG	0.02 ± 0.005	40 ± 17
dCTP	C	G	0.015 ± 0.002	310 ± 82
dCTP	C	3DG	0.030 ± 0.008	210 ± 120
dGTP	C	G	135 ± 4	21 ± 2
dGTP	C	3DG	0.45 ± 0.02	76 ± 19
dTTP	C	G	0.022 ± 0.002	42 ± 11
dTTP	C	3DG	0.02 ± 0.01	40 ± 15
dATP	G	G	0.308 ± 0.00123	53 ± 7
dATP	G	3DG	0.000015 ± 0.000004	61 ± 27
dCTP	G	G	55 ± 7	6 ± 3
dCTP	G	3DG	0.22 ± 0.01	76 ± 9
dGTP	G	G	0.056 ± 0.004	45 ± 10
dGTP	G	3DG	0.0033 ± 0.0002	5.0 ± 0.7
dTTP	G	G	0.034 ± 0.005	99 ± 40
dTTP	G	3DG	0.00008 ± 0.000008	110 ± 60
dATP	T	G	191 ± 18	5.4 ± 1.4
dATP	T	3DG	1.5 ± 0.2	76 ± 13
dCTP	T	G	0.043 ± 0.001	150 ± 120
dCTP	T	3DG	0.007 ± 0.006	250 ± 180
dGTP	T	G	0.86 ± 0.02	240 ± 93
dGTP	T	3DG	0.03 ± 0.01	330 ± 160
dTTP	T	G	0.012 ± 0.002	100 ± 41
dTTP	T	3DG	0.033 ± 0.005	100 ± 50

[a] The reactions were initiated by the addition of the dNTP and $MgCl_2$ to a premixed solution containing buffer, DNA, and polymerase. The buffer during the reaction was 50 mM Tris-HCl (pH 8.0), 5 mM $MgCl_2$, 5 mM DTT, and 100 μg/mL BSA at 25 °C. The concentration of the KF^- (100 nM) was in excess over the DNA (25 nM). The first-order rate constants were determined from time courses with at least five time points in duplicate. k_{pol} and K_d^{dNTP} were determined with eq 4 with at least seven concentrations of dNTP.

suggest that the Arg668-N3-guanine hydrogen bond occurs during correct base pair formation but not during mispair formation opposite C.

With G as the template base, misincorporation was 4400−75 000 less efficient that correct base pair formation primarily through a decrease in k_{pol} that was enhanced by a 10-fold increase in K_d^{dNTP} (Figure 8D). The G to 3DG-induced decrease in k_{pol} was observed with the correct dCTP (430-fold) as well as with dATP (20 000-fold) and dTTP (425-fold). However, the G to 3DG substitution reduced the k_{pol} only 17-fold while the K_d^{dNTP} decreased 10-fold for the misincorporation of dGTP. These results suggest that the Arg668-N3-guanine hydrogen bond occurs during correct incorporation of dCTP as well as mis-incorporation of dATP and dTTP but not during mis-incorporation of dGTP.

With T as the template base, incorporation of dATP was 10 000- to 300 000-fold favored over misincorporation by an increased k_{pol} coupled with a 20- to 50-fold increase in K_d^{dNTP} (Figure 8E). The G to 3DG substitution produced a 130-fold decrease in k_{pol} and a 14-fold increase in K_d^{dNTP} for the incorporation of dTTP. These changes were reduced for the misincorporation reactions. These results suggest that the Arg668-N3-guanine hydrogen bond occurs during correct incorporation of dATP but not during mispair formation.

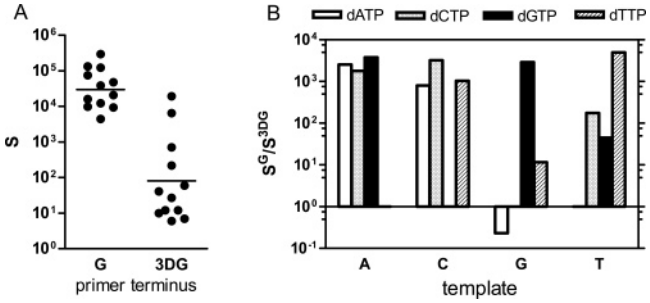

FIGURE 9: Decrease in fidelity due to the G to 3DG substitution at the primer terminus with oligodeoxynucleotides described in Figure 8. A. Plot of selectivity for G and 3DG at primer terminus. The lines are the geometric means, which for G is 32 000 and 3DG is 81. $S = (k_{pol}/K_d^{dNTP})^{correct}/(k_{pol}/K_d^{dNTP})^{mispair}$. B. Discrimination against specific mispair formation. The *Y*-axis represents the selectivity of the reaction with G divided by the selectivity of the reaction with 3DG at the primer terminus.

The G to 3DG substitution decreases the k_{pol} for the formation of the correct base pairs as well as most incorrect base pairs. However, the decrease in k_{pol} due to the G to 3DG substitution is less for mispair formation than for correct base pair formation. As a consequence, the fidelity of replication is less with 3DG at the primer terminus than with G.

The selectivity against mispair formation with G and 3DG at the primer terminus for the oligodeoxynucleotides in Figure 8 is shown in Figure 9A. The average selectivity with G at the primer terminus is 30 000. The selectivity against mispair formation with 3DG at the primer terminus ranges from 6 to 19 000. However only two of the values are > 1000, and the selectivity has a geometric mean of 80. The reduction of selectivity from 30 000 to 80 due to the G to 3DG substitution suggests that the hydrogen bond between Arg668 and the N3-position of the primer terminal guanine contributes significantly to the fidelity of the polymerase. Figure 9B shows that the effect of the G to 3DG substitution on the selectivity is dependent on the identity of the mis-incorporation. The incorporation of dATP opposite G is the differs from the other 11 mispairs in that the G to 3DG substitution enhances the selectivity of the reaction.

DISCUSSION

Use of 3DG To Probe Interactions with 3-Position of Guanine. The differences between guanine and 3DG do not prevent 3DG from being a substrate for DNA polymerases. Our present kinetic studies with KF^- as well of those with polymerase η (*41*) have shown that 3DG can replace G at several sites in the binding pocket with less than a 10-fold decrease in rate. With polymerase η, the largest decrease in rate (116-fold) occurs when 3dDGTP replaced dGTP as the incoming dNTP, while with KF^- the largest decrease in rate occurred with 3DG at the primer terminus. The high catalytic efficiency of **P1(3DG)** as a substrate for polymerase η suggests that the inefficiency of **P1(3DG)** as a substrate for KF^- is not due to its inherent unsuitability as a substrate but due to specific interactions between KF^- and the minor groove of the primer terminus.

Scheme 4: Potential G/C and G/T Interactions with Arg668

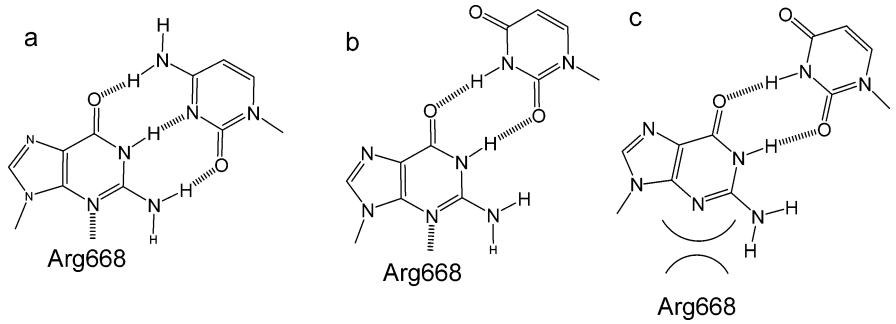

Interactions between E. coli DNA Polymerase I and the Minor Groove of DNA. Crystal structures of BF, *Taq* and T7 DNA polymerases (*10*−*12*), which are closely related proteins to KF$^-$, leads to the prediction that there are hydrogen bonds between Gln849 and T1, Arg668 and P1. In addition, the crystal structures of each protein show other interactions between other amino acid residues and the minor groove of DNA indicating that there may be hydrogen bonds from KF to other minor groove positions. The importance of Arg668 and Gln849 in catalysis have been supported by the reduced activities of the R668A and Q849A mutants (*14*, *42*). Moreover, Arg668 plays a role in maintaining fidelity of DNA replication while Gln849 does not (*43*). The use of adenine analogues, 9-methyl-1*H*-imidazo[(4,5)-*b*]pyridine and 4-methylbenzimidazole, to map the binding site of KF$^-$ indicated that the polymerase makes a functional contact with the minor groove of the primer terminus but not to the other positions (*22*, *23*). The observations that disruption of hydrogen bonds predicted by X-ray crystallography do not always affect the rate of reaction has led to labeling of the hydrogen bonds as structural (identified by crystallography) or functional (identified by kinetics) (*25*, *41*).

We examined interactions between the polymerase and the DNA by using the more conservative guanine to 3DG substitution (Scheme 1). We found that changing G to 3DG at the P1 position reduced the k_{pol}/K_d^{dNTP} approximately 400-fold while substitutions at the other positions generally decreased the rate less than 12-fold. Our results are consistent with the results of Morales and Kool (*22*, *23*). From these data, we conclude that there is a functional hydrogen bond between Arg668 and P1 position and if a hydrogen bond was made to the T1 or any other positions, they do not impact the transition state of the rate-limiting step of the reaction.

Mechanism by which Arg668−*Primer Terminus*−*Minor Groove Interaction Influences Rate.* The reduction in rate of reaction with 3DG at P1 may be due to the decreased rate of one or more steps in the reaction pathway. Since a burst was not observed with 3DG at P1, the rate-limiting step may be substrate binding (k_1 or k_2), the conformational change (k_3) or phosphodiester bond formation (k_4). It is unlikely that the rate of substrate binding would be rate limiting since the rates of KF$^+$ binding to unmodified DNA and dNTP are diffusion controlled (*37*, *44*). However, reduced binding of the DNA may alter the concentration of the DNA-KF$^-$ complex that would react with the dNTP to produce a burst. We found that the G to 3DG substitution at any position in the DNA only slightly affected the K_d^{dNTP} or the K_d^{DNA}. And thus, the binding affinity of the DNA or dNTP is not the cause of the decreased rate of replication with **P1(3DG)**. Consequently reduction in either k_3 or k_4 is responsible for the reduced rate of reaction.

Scheme 5: Potental G/A Interactions with KF−

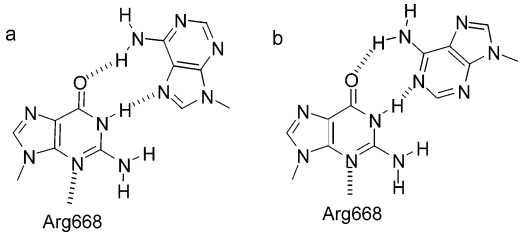

Fidelity of Mispair Extension. One mechanism by which polymerases replicate DNA with high fidelity is by preferentially extending Watson−Crick base pairs more efficiently than mispairs. The slower extension of a mispair would allow a proofreading exonuclease activity to excise the incorrect base pair. Our results in Figure 7 show that the hydrogen bond between Arg668 and the N3-position of guanine exists and is important during the rate-limiting step of the extension past the G/C base pair as well as the G/A and G/G mispairs but not the G/T mispair. The loss of a selectivity to prevent extension of G/T mispair is consistent with the results that R668A is not as good as wild-type in preventing the extension of G/T mispairs (*18*) The formation of this hydrogen bond, or actually the lack of this hydrogen bond in the mispair, may be the mechanism by which KF$^-$ selects against the extension of the G/T mispair.

BF crystals are catalytically active and correct base pairs as well as mispairs can be formed by these crystals. The G/T mismatch, obtained by extension of the DNA in the presence of Mn^{2+} and dGTP, was found bound to the polymerase at the post-insertion site, which corresponds to the P1/T1 position in our terminology. In the binary complex, the protein adopts an open conformation in which the newly incorporated guanine is in a conformation similar to that of a cognate base at that position. Consequently, compared with the complex with the G/C base pair (Scheme 4a), the positions of the 3′-hydroxyl and the hydrogen bond between Arg and the N3-position of the guanine are the same, while the position of the template base is significantly distorted, positioned toward the DNA major groove (Scheme 4b) (*45*). If this were the structure during phosphodiester bond formation we would expect the G to 3DG substitution to decrease the rate of reaction. Our results are more consistent with a structure such as Scheme 4c in which the hydrogen bond between Arg668 and the base is broken. The movement of guanine toward the minor groove could disrupt the hydrogen bond to Arg668, either by preventing the bond from forming or altering its location.

Scheme 6: Potential G/G Interactions with KF−

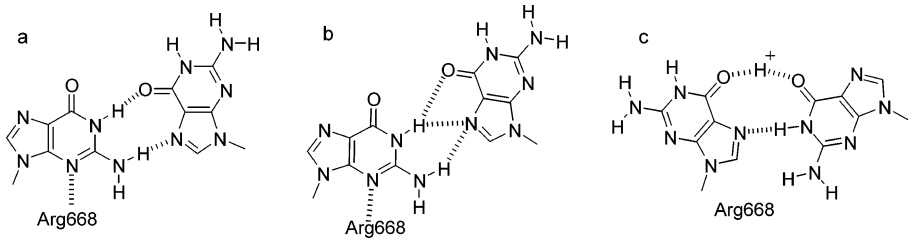

Our kinetic results indicate the presence of a hydrogen bond during the extension of G/A mispairs. The presence of the hydrogen bond would require the guanine on the primer terminus to be in the anti conformation. Potential G/A complexes illustrated in Scheme 5 have been observed in oligodeoxynucleotides (*46*−*50*). The structure in Scheme 5a has the template dA to be in the syn conformation with Hoogsteen hydrogen bonding wit he G on the primer strand (*48*−*50*). In Scheme 5b, the adenine on the template is in the anti conformation and would cause the distance between the deoxyribose moieties to lengthen (*46*, *47*). A purine/purine mismatch in which one nucleotide is in the syn and the other in the anti conformation allows the mismatch to form a complex in which the helical width is much closer to a Watson−Crick base pair than is observed in the anti-anti structures. The BF crystals catalyzed the formation of the G/A base pair, but the DNA strands separated and the hydrogen bond complex between the dA and dG was not observed (*45*). Neither of these complexes in Scheme 5 appears to be optimal for DNA replication. Despite the presence of the minor groove hydrogen bond, there are many other differences between these structures and the classic Watson−Crick structure that the polymerase may use to slow the extension of the G/A mispair.

Our kinetic results also indicate the presence of a hydrogen bond during the extension of G/G mispairs. Scheme 6a and b show potential G/G-Arg669 complexes with base pairs that have been observed in oligodeoxynucleotides (*51*). The presence of a hydrogen bond between the primer guanine and Arg668 requires the guanine at the primer terminus to be in the anti conformation. Both structures have the template G in the syn conformation with slightly different hydrogen bonding structures. The structure of the G/G complex found in the crystallography experiments with BF is that in Scheme 6c in which the primer G is in the syn conformation while the template G is in the anti conformation. The difference between our result and the crystallography experiments (*45*) may indicate that the G/G mispair is formed with the incoming dNTP in the syn orientation and the template in the anti conformation, but that extension occurs with the primer G in the anti conformation and the template G in the syn conformation.

Fidelity of Mispair Formation. During correct base pair formation, the hydrogen bond between one imino group of Arg668 and the primer terminus positions the other imino group of Arg668 to align the deoxyribose of the incoming dNTP such that the α-phosphate can react with the 3′-hydroxyl of the primer (Figure 1). The G to 3DG substitution at the primer terminus reduces the rate of replication because the primer terminus-Arg668 hydrogen bond is broken and therefore Arg668 is not in position to align the incoming dNTP. During mispair formation, the G to 3DG substitution decreases k_{pol} to a much lesser degree than during correct base pair formation. These results indicate that the hydrogen bond between Arg668 and the minor groove of the primer terminus is not present, not as strong, or not as important during mispair formation as during correct base pair formation.

Our studies are consistent with a mechanism in which the newly forming mispair distorts the minor groove hydrogen bonding complex such that at least primer terminus branch of the Arg668 fork is lost. It is not known whether the hydrogen bond between Arg668 and the incoming dNTP is retained during mispair formation. If the Arg668 hydrogen bond fork between the primer terminus and the incoming dNTP is formed, it is not along the reaction pathway but would be a nonproductive complex.

The importance of the Arg668 fork, however, is dependent on the identity of the mispair. In the most extreme case, the G to 3DG substitution actually reduces the incorporation of dATP opposite G to a greater extent than dCTP opposite G. This result suggests that the Arg668 hydrogen bonding fork is operating in the formation of the A/G base pair. The reduced rate of incorporation of dATP opposite G must be due to other mechanisms.

CONCLUSIONS

DNA polymerases catalyzed phosphodiester bond formation proceeds through a nucleophilic substitution reaction that proceeds through a pentacoordinated α-phosphate transition state. For this reaction to proceed rapidly the 3′-hydroxyl nucleophile must be in-line with the α-phosphate and pyrophosphate leaving group. Arg668 can play an essential role in catalysis and fidelity of DNA replication by acting as a fulcrum between the incoming dNTP and primer terminus. When the terminal and nascent base pairs have Watson−Crick geometries then Arg668 can form hydrogen bonds to the minor groove of the primer terminus and the ring oxygen of the incoming dNTP as illustrated in Figure 1. By these interactions Arg668 can align the α-phosphate of the incoming dNTP with the 3′-hydroxyl such that reaction rapidly occurs. However with some mispairs at the terminal base pair or the newly forming base pair, the hydrogen bonding fork either does not form or it forms but misdirects the incoming dNTP into a sub-optimal and less reactive position. Mispair formation or extension would use other more energetic pathways that do not involve hydrogen bonds between Arg668 and the minor groove of the primer terminus.

SUPPORTING INFORMATION AVAILABLE

Three figures describing (1) chemical shifts for the protons bound to the *N*1 and *N*2-positions of 3DG and the *N*4-

position of cytosine at various ratios of 3DG and C, (2) UV spectroscopy of the thermal denaturation of oligodeoxynucleotide duplexes containing 3DG, and (3) pH dependence on the UV spectrum of 3DG. This material is available free of charge via the Internet at http://pubs.acs.org.

REFERENCES

1. Petruska, J., Goodman, M. F., Boosalis, M. S., Sowers, L. C., Cheong, C., and Tinoco, I., Jr. (1988) Comparison between DNA melting thermodynamics and DNA polymerase fidelity, *Proc. Natl. Acad. Sci., U.S.A. 85*, 6252−6256.
2. Echols, H., and Goodman, M. F. (1991) Fidelity mechanisms in DNA replication, *Annu. Rev. Biochem. 60*, 477−511.
3. Goodman, M. F. (1997) Hydrogen bonding revisited: geometric selection as a principal determinant of DNA replication fidelity, *Proc. Natl. Acad. Sci., U.S.A. 94*, 10493−10495.
4. Petruska, J., Sowers, L. C., and Goodman, M. F. (1986) Comparison of nucleotide interactions in water, proteins, and vacuum: model for DNA polymerase fidelity, *Proc. Natl. Acad. Sci., U.S.A. 83*, 1559−1562.
5. Kool, E. T. (2002) Active site tightness and substrate fit in DNA replication, *Annu. Rev. Biochem. 71*, 191−219.
6. Kennard, O., and Salisbury, S. A. (1993) Oligonucleotide X-ray structures in the study of conformation and interactions of nucleic acids, *J. Biol. Chem. 268*, 10701−10704.
7. Seeman, N. C., Rosenberg, J. M., and Rich, A. (1976) Sequence-specific recognition of double helical nucleic acids by proteins, *Proc. Natl. Acad. Sci., U.S.A. 73*, 804−808.
8. Brown, T., and Kennard, O. (1992) Structural basis of DNA mutagenesis, *Curr. Opin. Struct. Biol. 2*, 354−360.
9. Pelletier, H., Sawaya, M. R., Kumar, A., Wilson, S. H., and Kraut, J. (1994) Structures of ternary complexes of rat DNA polymerase beta, a DNA template-primer, and ddCTP, *Science 264*, 1891−1903.
10. Kiefer, J. R., Mao, C., Braman, J. C., and Beese, L. S. (1998) Visualizing DNA replication in a catalytically active *Bacillus* DNA polymerase crystal, *Nature 391*, 304−307.
11. Li, Y., Korolev, S., and Waksman, G. (1998) Crystal structures of open and closed forms of binary and ternary complexes of the large fragment of *Thermus aquaticus* DNA polymerase I: structural basis for nucleotide incorporation, *EMBO J. 17*, 7514−7525.
12. Doublie, S., Tabor, S., Long, A. M., Richardson, C. C., and Ellenberger, T. (1998) Crystal structure of a bacteriophage T7 DNA replication complex at 2.2 Å resolution, *Nature 391*, 251−258.
13. Beard, W. A., Osheroff, W. P., Pradad, R., Sawaya, M. R., Jaju, M., Wood, T. G., Kraut, J., Kunkel, T. A., and Wilson, S. H. (1996) Enzyme-DNA interactions required for efficient nucleotide incorporation and discrimination in human DNA polymerase beta, *J. Biol. Chem. 271*, 12141−12144.
14. Polesky, A. H., Dahlberg, M. E., Benkovic, S. J., Grindley, N. D. F., and Joyce, C. M. (1992) Side chains involved in catalysis of polymerase reaction of DNA polymerase I from *Escherichia coli*, *J. Biol. Chem. 267*, 8417−8428.
15. Werneburg, B. G., Ahn, J., Zhong, X., Hondal, R. J., Kraynov, V. S., and Tsai, M. D. (1996) DNA polymerase beta: pre-steady-state kinetic analysis and roles of arginine-283 in catalysis and fidelity, *Biochemistry 35*, 7041−7050.
16. Ahn, J., Werneburg, B. G., and Tsai, M. D. (1997) DNA polymerase beta: structure-fidelity relationship from pre-steady-state kinetic analyses of all possible correct and incorrect bases pairs for wild type and R283A mutant, *Biochemistry 36*, 1100−1107.
17. Osheroff, W. P., Beard, W. A., Wilson, S. H., and Kunkel, T. A. (1999) Base substitution specificity of DNA polymerase beta depends on interactions in the DNA minor groove, *J. Biol. Chem. 274*, 20749−20752.
18. Minnick, D. T., Bebenek, K., Osheroff, W. P., Turner, R. M., Jr., Astatke, M., Liu, L., Kunkel, T. A., and Joyce, C. M. (1999) Side chains that influence fidelity at the polymerase active site of *Escherichia coli* DNA polymerase I (Klenow fragment), *J. Biol. Chem. 274*, 3067−3075.
19. Cosstick, R., Li, X., Tuli, D. K., Williams, D. M., Connolly, B. A., and Newman, P. C. (1990) Molecular recognition in the minor groove of the DNA helix. Studies on the synthesis of oligonucleotides and polynucleotides containing 3-deaza-2′-deoxyadenosine. Interaction of the oligonucleotides with the restriction endonuclease *Eco*RV, *Nucleic Acids Res. 18*, 4771−4778.
20. Hendrickson, C. L., Devine, K. G., and Benner, S. A. (2004) Probing minor groove recognition contacts by DNA polymerases and reverse transcriptases using 3-deaza-2′-deoxyadenosine, *Nucleic Acids Res. 32*, 2241−2250.
21. Spratt, T. E. (1997) Enzyme-nucleotide interactions during DNA replication, *Biochemistry 36*, 13292−13297.
22. Morales, J. C., and Kool, E. T. (1999) Minor groove interactions between polymerases and DNA: more essential to replication than Watson−Crick hydrogen bonds? *J. Am. Chem Soc. 121*, 2323−2324.
23. Morales, J. C., and Kool, E. T. (2000) Varied molecular interactions at the active sites of several DNA polymerases: nonpolar nucleoside isosteres as probes, *J. Am. Chem Soc. 122*, 1001−1007.
24. Guo, M. J., Hildbrand, S., Leumann, C. J., McLaughlin, L. W., and Waring, M. J. (1998) Inhibition of DNA polymerase reactions by pyrimidine nucleotide analogues lacking 2-keto group, *Nucleic Acids Res. 26*, 1863−1869.
25. Morales, J. C., and Kool, E. T. (2000) Functional hydrogen-bonding map of the minor groove binding tracks of six DNA polymerases, *Biochemistry 39*, 12979−12988.
26. Spratt, T. E. (2001) Identification of hydrogen bonds between *Escherichia coli* DNA polymerase I (Klenow fragment) and the minor groove of DNA by amino acid substitution of the polymerase and atomic substitution of the DNA, *Biochemistry 40*, 2647−2652.
27. Meyer, A. S., Blandino, M., and Spratt, T. E. (2004) E. coli DNA polymerase I (Klenow fragment) uses a hydrogen bonding fork from Arg668 to the primer terminus and incoming deoxynucleotide triphosphate to catalyze DNA replication, *J. Biol. Chem. 279*, 33043−33046.
28. Dunn, D. B., and Hall, R. H. (1986) in *Handbook of Biochemistry and Molecular Biology* (Fasman, G. D., Ed.) pp 65−215, CRC Press, Boca Raton, FL.
29. Spratt, T. E., and Campbell, C. R. (1994) Synthesis of oligodeoxynucleotides containing analogues of O^6-methylguanine and reaction with O^6-alkylguanine-DNA alkyltransferase, *Biochemistry 33*, 11364−11371.
30. Borer, P. (1977) Optical properties of nucleic acids, absorption, and circular dichroism spectra, in *Handbook of Biochemistry and Molecular Biology* (Fasman, G. D., Ed.) p 589, CRC Press, Boca Raton, FL.
31. Ogilvie, K. K. (1983) The alkylsilyl protecting groups: in particular, the *tert*-butyldimethylsilyl group in nucleoside and nucleotide chemistry, in *Nucleosides, nucleotides, and their biological applications* (Rideout, J. L., Henry, D. W., Beacham, L. M., III, Eds.) pp 209−256, Academic Press, Inc., New York.
32. Katz, L., and Penman, S. (1966) Association by hydrogen bonding of free nucleosides in nonaqueous solution, *J. Mol. Biol. 15*, 220−231.
33. Williams, L. D., and Shaw, B. R. (1987) Protonated base pairs explain the ambiguous pairing properties of O^6-methylguanine, *Proc. Natl. Acad. Sci., U.S.A. 84*, 1779−1783.
34. Dugas, H., and Penney, C. (1981) Bioorganic chemistry of the phosphates, in *Bioorganic Chemistry* (Cantor, C. R., Ed.) pp 93−178, Springer-Verlag, New York.
35. Chen, J., McAllister, M. A., Lee, J. K., and Houk, K. N. (1998) Short, strong hydrogen bonds in the gas phase and in solution: Theoretical exploration of pK_a matching and environmental effects on the strengths of hydrogen bonds and their potential roles in enzymic catalysis, *J. Org. Chem. 63*, 4611−4619.
36. Larson, J. W., and McMahon, T. B. (1983) Strong hydrogen bonding in gas-phase anions. An ion cyclotron resonance determination of fluoride binding energetics to Broensted acids from gas-phase fluoride exchange equilibrium measurements, *J. Am. Chem Soc. 105*, 2944−2950.
37. Kuchta, R. D., Mizrahi, V., Benkovic, P. A., Johnson, K. A., and Benkovic, S. J. (1987) Kinetic mechanism of DNA polymerase I (Klenow), *Biochemistry 26*, 8410−8417.
38. Kuchta, R. D., Benkovic, P., and Benkovic, S. J. (1988) Kinetic mechanisms whereby DNA polymerase I (Klenow) replicates DNA with high fidelity, *Biochemistry 27*, 6717−6725.
39. Mizrahi, V., Henrie, R. N., Marlier, J. F., Johnson, K. A., and Benkovic, S. J. (1985) Rate-limiting steps in the DNA polymerase I reaction pathway, *Biochemistry 24*, 4010−4018.
40. Lowe, L. G., and Guengerich, F. P. (1996) Steady-state and pre-steady-state kinetic analysis of dNTP insertion opposite 8-oxo-

7,8-dihydroguanine by *Escherichia coli* polymerase I exo$^-$ and II exo$^-$, *Biochemistry 35*, 9840−9849.
41. Washington, M. T., Wolfle, W. T., Spratt, T. E., Prakash, L., and Prakash, S. (2003) Yeast DNA polymerase eta makes functional contacts with the DNA minor groove only at the incoming nucleoside triphosphate, *Proc. Natl. Acad. Sci. U.S.A. 100*, 5113−5118.
42. Polesky, A. H., Steitz, T. A., Grindley, N. D. F., and Joyce, C. M. (1990) Identification of residues critical for the polymerase activity of the Klenow fragment of DNA polymerase I from *Escherichia coli*, *J. Biol. Chem. 265*, 14579−14591.
43. Minnick, D. T., Liu, L., Grindley, N. D. F., Kunkel, T. A., and Joyce, C. M. (2002) Discrimination against purine-pyrimidine mispairs in the polymerase active site of DNA polymerase I: A structural explanation, *Proc. Natl. Acad. Sci., U.S.A. 99*, 1194−1199.
44. Eger, B. T., Kuchta, R. D., Carroll, S. S., Benkovic, P. A., Dahlberg, M. E., Joyce, C. M., and Benkovic, S. J. (1991) Mechanism of DNA replication fidelity for three mutants of DNA polymerase I: Klenow fragment KF(exo+), KF(polA5), and KF(exo-), *Biochemistry 30*, 1441−1448.
45. Johnson, S. J., and Beese, L. S. (2004) Structures of mismatch replication errors observed in a DNA polymerase, *Cell 116*, 803−816.
46. Kan, L. S., Chandrasegaran, S., Pulford, S. M., and Miller, P. S. (1983) Detection of a guanine X adenine base pair in a decadeoxyribonucleotide by proton magnetic resonance spectroscopy, *Proc. Natl. Acad. Sci U.S.A. 80*, 4263−4265.
47. Prive, G. G., Heinemann, U., Chandrasegaran, S., Kan, L. S., Kopka, M. L., and Dickerson, R. E. (1987) Helix geometry, hydration, and G.A mismatch in a B-DNA decamer, *Science 238*, 498−504.
48. Webster, G. D., Sanderson, M. R., Skelley, J. V., Neidle, S., Swann, P. F., Li, B. F. L., and Tickle, I. J. (1990) Crystal structure and sequence-dependent conformation of the A−G mispaired oligonucleotide d(CGCAAGCTGGCG), *Proc. Natl. Acad. Sci., U.S.A. 87*, 6693−6697.
49. Hunter, W. N., Brown, T., and Kennard, O. (1986) Structural features and hydration of d(C-G-C-G-A-A-T-T-A-G-C-G); a double helix containing two G.A mispairs, *J. Biomol. Struct. Dyn. 4*, 173−191.
50. Brown, T., Hunter, W. N., Kneale, G., and Kennard, O. (1986) Molecular structure of the G.A base pair in DNA and its implications for the mechanism of transversion mutations, *Proc. Natl. Acad. Sci U.S.A. 83*, 2402−2406.
51. Skelly, J. V., Edwards, K. J., Jenkins, T. C., and Neidle, S. (1993) Crystal structure of an oligonucleotide duplex containing G.G base pairs: influence of mispairing on DNA backbone conformation, *Proc. Natl. Acad. Sci., U.S.A. 90*, 804−808.

BI047460F